

Adhesion of Elastic Thin Films: Double Peeling of Tapes Versus Axisymmetric Peeling of Membranes

L. Afferrante · G. Carbone · G. Demelio ·
N. Pugno

Received: 18 April 2013 / Accepted: 16 September 2013 / Published online: 1 October 2013
© Springer Science+Business Media New York 2013

Abstract The mechanism of detachment of thin films from a flat smooth rigid substrate is investigated. In particular, analytical solutions in closed form are proposed for the double peeling of an elastic tape as well as for the axisymmetric peeling of a membrane. We show that in the case of double peeling of an endless elastic tape, a critical value of the pull-off force is found, above which the tape is completely detached from the substrate. In particular, as the detachment process advances, the peeling angle is stabilized on a limiting value, which only depends on the geometry of the tape, its elastic modulus and on the interfacial energy $\Delta\gamma$. This predicted behavior agrees with the “theory of multiple peeling” and clarifies some aspects of this theory. Moreover, it is also corroborated by experimental results (work in progress) we are carrying out on a standard adhesive tape adhered to a smooth flat poly(methyl methacrylate) surface. In the case of the axisymmetric adhering membrane, a different behavior is observed. In such case, the system is always stable, and the detached area monotonically increases with the peeling force, i.e., the elastic membrane can sustain

in principle any applied force. Results are validated by a fully numerical analysis performed with the aid of a finite element commercial software.

Keywords Peeling · Double peeling · Peeling of thin membranes · Fracture · Adhesion · Energy release rate

1 Introduction

Adhesion of thin films and membranes is crucial in a countless number of biological and industrial applications. As an example, the membrane–membrane adhesion is important in the mechanism of aggregation of cells and in the attachment of cells to extracellular matrix (ECM). Cellular adhesion is also essential in maintaining multicellular structure. The cell adhesion theory, known as *differential adhesion hypothesis*, was developed in the 1960s by Steinberg [1–3]. It is based on the assumptions that adhesion of cells occurs as a result of surface tensions due to embryonic tissues and cell lines. This theory explains “the mechanism by which heterotypic cells in mixed aggregates sort out into isotypic territories” and is generally supposed “to be sufficient to account for the phenomenon without the need to postulate cell type specific adhesion systems” [4].

An other example is the hairy attachment systems of insects, reptiles and spiders that show extraordinary adhesive abilities [5] even at the human size scale [6, 7]. These systems consist of arrays of hierarchical hairs or setae, which allow for a large contact area and hence high adhesion derived from van der Waals interaction forces [8]. The single peeling model of Kendall [9] has been used to explain why most biological hairy adhesive systems involved in

L. Afferrante (✉) · G. Carbone · G. Demelio
TriboLAB, Department of Mechanics, Mathematics and Management (DMMM), Politecnico of Bari, V.le Japigia, 185 Bari, Italy
e-mail: l.afferrante@poliba.it
URL: <http://tribolab.poliba.it>

N. Pugno
Laboratory of Bio-inspired and Graphene Nanomechanics, Department of Civil, Environmental and Mechanical Engineering, University of Trento, Via Mesiano 77, 38123 Trento, Italy

N. Pugno
Center for Materials and Microsystems, Fondazione Bruno Kessler, Via Sommarive 18, 38123 Povo (Trento), Italy

locomotion rely on spatula-shaped terminal elements [10]. Indeed, many insects, spiders and some vertebrates are capable of climbing on diverse substrates, using adhesive structures on their legs [11]. In this respect, the role of highly flexible terminal spatula elements as compliant contacting surfaces is crucial [12, 13]. An additional example is collapse and sticking of thin films onto substrates that are serious problems in microfabrication and operation processes of microelectromechanical systems (MEMS) [14, 15]. In particular, at separations of the order of a micrometer, occurrence of sticking phenomena has been reported, wherein a thin micromachined membrane unexpectedly glues on an adjacent parallel surface [16]. Sticking is usually observed in wet environment; however, it also occurs in vacuum. In this case, van der Waals forces [17, 18] are often responsible for sticking in MEMS.

For these reasons, many experimental and theoretical approaches have been developed to study the mechanism of detachment of adhering systems such as thin films [19–27]. In Ref. [22], for example, a comprehensive study of the detachment process of a rigid flat punch from a flexible membrane is proposed under the assumption of small deformations. The model has been extended to the case of isotropic incompressible hyperelastic membranes in [28], showing that finite deformations can have a significant effect on membrane adhesion. In [29], moving from the method developed in [30], analytical solutions for neo-Hookean material and an I_2 -based material model are given in the limiting case of large membrane strain due to strong adhesion or large pre-stretch.

The study of the detachment of thin adhesive films also allows to elucidate some of the mechanisms of gecko adhesion. In fact, in order to avoid toe detachment, the gecko adhesive mechanism is based on the use of opposing feet and toes leading to a V-shaped geometry [31–36], whose behavior strongly resembles the multiple peeling mechanism studied in [37]. Moreover, bio-inspired micropatterned surfaces [38], showing enhanced adhesive [5, 39, 40], and/or superhydrorepellent [41–44] properties, have been drawing a strong scientific interest. The potential applications of gecko like adhesives in robotics, biomedical devices, manufacturing and consumer products have spawned a large number of attempts to create usable material [45]. For this reason, many experimental [32, 34, 46–48], computational [31, 49, 50] and theoretical [7, 10, 37, 51–58], investigations have been carried out to achieve a better understanding of biological attachment/detachment mechanisms, also in the presence of roughness. For example, in [59], the work of [60] was extended to the case of adhesive contact between two rough surfaces. However, recently it has been shown [61–65] that the so-called multiasperity contact models do not give reliable results, and hence, a deep understanding of the adhesion phenomena is still lacking.

In this paper, we study the double peeling of an endless thin tape and the axisymmetric peeling of a circular initially flat elastic membrane adhering to a rigid substrate. We find that, in the case of tape detachment, the peeling angle is always stabilized on a limiting value and the supported load cannot exceed a maximum beyond which the endless tape necessarily detaches from the substrate. This predicted behavior is in agreement with the theory of multiple peeling [37] and with experimental observations. In the case of thin membranes, instead, there is no limit, in principle, to the load that can be supported by the system.

2 Formulation

Consider an adhesive tape or the adhesive membrane in partial contact with a flat rigid substrate. The non-contact area acts as an interfacial crack, that, as the system is pulled apart from the substrate, propagates determining the advance of the peeling process. Observe that, in the case of the axisymmetric membrane, the peeling line is a circumference whose radius increases as the crack propagates outwards, while in the tape case, the length of peeling line remains constant during the detachment process. Both tape and membrane are assumed to be elastic and nearly incompressible with Young's modulus $E = 3$ MPa and Poisson's ratio $\nu = 0.5$. Moreover, we assume that, during the detachment process, suction effects can be neglected. Assuming isothermal conditions, the equilibrium requires that the total free energy U_{tot} is stationary (Griffith criterion), i.e.,

$$G = \Delta\gamma \quad (1)$$

where $\Delta\gamma$ is the work of adhesion, also referred to as the Duprè energy of adhesion [66], and G is the energy release rate at the crack tip, defined as

$$G = -\left(\frac{\partial U_{\text{el}}}{\partial S}\right)_{\delta} \quad (2)$$

when the displacement δ is prescribed, or

$$G = -\left(\frac{\partial U_{\text{el}}}{\partial S} + \frac{\partial U_P}{\partial S}\right)_P \quad (3)$$

when the external load P is fixed. In Eqs. 2 and 3, U_{el} is the elastic energy stored in the system, U_P is the potential energy associated with the force P and S is the size of the detached area.

2.1 Double Peeling of an Elastic Tape

Now, consider an elastic tape, with cross-section $A_t = bt$, pulled apart from a rigid substrate by a constant vertical

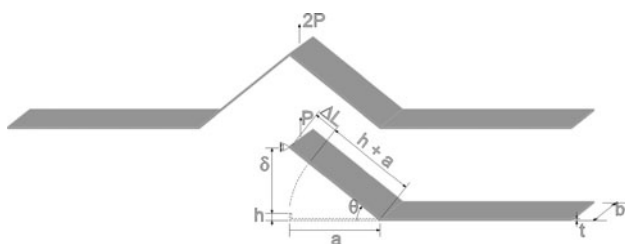


Fig. 1 Double peeling of a tape

force $2P$, as shown in Fig. 1. Due to the symmetry of the system, we can limit our study to half the tape.

The action of the vertical force P makes the tape increase its length of the quantity

$$\Delta L = \frac{(a + h)T}{E^*bt} \tag{4}$$

where $T = P / \sin \theta$ and $E^* = E / (1 - \nu^2)$ is the composite Young’s modulus. We assume b is sufficiently large to consider the tape in plane strain conditions. Therefore, the elastic energy is

$$U_{el} = \frac{1}{2}T\Delta L = \frac{1}{2} \frac{P^2(a + h)}{E^*bt \sin^2 \theta} \tag{5}$$

and the potential energy associated with the applied load P is

$$U_P = -P(a + h + \Delta L) \sin \theta = -P(a + h) \left(\sin \theta + \frac{P}{E^*bt} \right) \tag{6}$$

The energy release rate G can be then obtained from (3) as

$$G = -\frac{1}{b} \left(\frac{\partial U_{el}}{\partial a} + \frac{\partial U_P}{\partial a} \right)_P = \frac{P}{b \sin \theta} \left(\frac{P}{2E^*bt \sin \theta} + 1 - \cos \theta \right) \tag{7}$$

where we have used that $a = (a + h + \Delta L) \cos \theta$, (see Fig. 1), i.e., that

$$\frac{h}{a} = \frac{1 - \cos \theta - P \cot \theta / (E^*bt)}{\cos \theta + P \cot \theta / (E^*bt)} \tag{8}$$

The corresponding vertical displacement δ is

$$\delta = -\left(\frac{\partial U_{el}}{\partial P} + \frac{\partial U_P}{\partial P} \right)_a = h \left[\frac{P / (E^*bt) + \sin \theta}{1 - \cos \theta - P \cot \theta / (E^*bt)} - 1 \right] \tag{9}$$

Interestingly, recalling that $T = P / \sin \theta$, we note that Eq. (7) is exactly the same as the one obtained by Kendall [9] as previously demonstrated in [37]. It clearly indicates that, at equilibrium (i.e., when $G = \Delta\gamma$), the load P only depends on the peeling angle θ . However, for the double

peeling case, a lower bound θ_{lim} of the peeling angle exists below which any equilibrium solution, predicted by the Griffith criterion, is not physically meaningful (see also Sect. 3.1). In fact, observing that $h/a \geq 0$, Eq. (8) implies that at equilibrium, the peeling angle must satisfy the condition

$$1 - \cos \theta - \frac{P}{E^*bt} \cot \theta \geq 0, \tag{10}$$

i.e., $\theta \geq \theta_{lim}$, where θ_{lim} is solution of the equation $1 - \cos \theta - P \cot \theta / (E^*bt) = 0$.

A convenient dimensionless formulation can be developed by defining the following quantities

$$\hat{\delta} = \delta/h; \quad \hat{a} = a/h; \quad \hat{P} = P / (E^*bt); \quad \hat{G} = G / (E^*t) \tag{11}$$

in which case Eqs. 7 and 9 reduce to

$$\hat{G} = \frac{\hat{P}}{\sin \theta} \left(\frac{\hat{P}}{2 \sin \theta} + 1 - \cos \theta \right) \tag{12}$$

$$\hat{\delta} = \frac{\hat{P} + \sin \theta}{1 - \cos \theta - \hat{P} \cot \theta} - 1 \tag{13}$$

2.2 Axisymmetric Peeling of an Elastic Membrane:

A Simplified approach

Now consider a membrane, pulled apart by applying a vertical displacement δ , as shown in Fig. 2. The total force P acting on the membrane is balanced by the vertical component (perpendicular to the flat substrate) of the resulting force, due to membrane traction stresses σ_m ,

$$P = 2\pi r t \sigma_m \sin \theta \tag{14}$$

We assume negligible radial displacement w as well as negligible circumferential strain ϵ_θ . As a result, the only component of the membrane strain is the radial strain

$$\epsilon_m = \frac{dl - dr}{dr} = \sqrt{1 + u'(r)^2} - 1 \simeq \frac{u'(r)^2}{2} \tag{15}$$

where $u(r)$ is the vertical displacement (i.e., perpendicular to the flat substrate) of the membrane. The stress is therefore

$$\sigma_m = E^* \epsilon_m = \frac{1}{2} E^* u'(r)^2 \tag{16}$$

Substituting (16) in (14), $u(r)$ can be obtained by solving the following ordinary differential equation

$$u'(r)^3 = -\frac{P / (\pi E^*t)}{r} \tag{17}$$

with the boundary condition $u(r_0 + a) = 0$, being a the detached radius. Since we are controlling the displacement δ , the unknown load P can be determined enforcing the

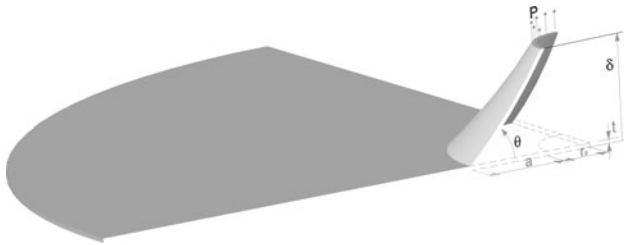


Fig. 2 Peeling of an axisymmetric initially flat membrane

additional boundary condition $u(r_0) = \delta$. Solving Eq. (17) with the aforementioned boundary conditions yields:

$$u(r) = \delta \frac{r^{2/3} - (r_0 + a)^{2/3}}{r_0^{2/3} - (r_0 + a)^{2/3}} \tag{18}$$

and

$$P = \frac{8\pi E^* t \delta^3}{27 [(r_0 + a)^{2/3} - r_0^{2/3}]^3} \tag{19}$$

Note that Eq. (19) is the equation of state of the system, which correlates the displacement δ , the load P and the radius a of the detached area. The total elastic energy can be calculated as

$$U_{el} = \frac{1}{2} \int_V (\sigma_m \varepsilon_m + \sigma_\theta \varepsilon_\theta) dV \approx \frac{1}{2} \int_V \frac{\sigma_m^2}{E^*} dV = \frac{2\pi E^* t \delta^4}{27 [(r_0 + a)^{2/3} - r_0^{2/3}]^3} \tag{20}$$

The energy release rate G can be hence obtained from (2) as

$$G = -\frac{1}{2\pi(r_0 + a)} \left(\frac{\partial U_{el}}{\partial a} \right)_\delta = \frac{2\pi E^* t \delta^4}{27 (r_0 + a)^{4/3} [(r_0 + a)^{2/3} - r_0^{2/3}]^4} \tag{21}$$

Finally, the detached radius at the equilibrium can be obtained by enforcing the Griffith condition (1).

By defining the following reduced quantities

$$\hat{\delta} = \delta/r_0; \quad \hat{a} = a/r_0; \quad \hat{P} = P/(2\pi E^* r_0 t); \quad \hat{G} = G/(E^* t) \tag{22}$$

Eqs. (19) and (21) can be rewritten in dimensionless form as

$$\hat{P} = \frac{4\hat{\delta}^3}{27 [(1 + \hat{a})^{2/3} - 1]^3} \tag{23}$$

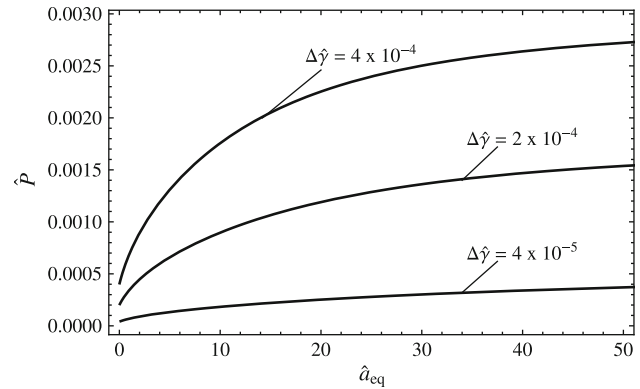


Fig. 3 The dimensionless peeling force \hat{P} as a function of the dimensionless detached length \hat{a}_{eq} for an adhesive tape. Plots are given for different values of the dimensionless work of adhesion $\Delta\hat{\gamma}$

$$\hat{G} = \frac{2\hat{\delta}^4}{27(1 + \hat{a})^{4/3} [(1 + \hat{a})^{2/3} - 1]^4} \tag{24}$$

3 Results and Discussion

In this section, we compare the double peeling of an endless tape with the axisymmetric peeling of a membrane. As we will show in the sequel, the two adhesive mechanisms are very different from each other. In particular, in the double peeling case, the dimensionless load per unit length of the peeling line, that the tape can support, cannot exceed a maximum value uniquely identified by the dimensionless quantity $\Delta\hat{\gamma} = \Delta\gamma/(E^*t)$. On the other hand, in the case of the axisymmetric peeling of an infinite membrane, this limiting load does not exist, i.e., the membrane can support any load, independently of how large it is. This indeed can be easily understood if one considers that the supported load P at equilibrium should be proportional to the length of the peeling line. So, in the case of the tape, the peeling line does not change during the peeling process, whereas in the case of the membrane, the peeling line is just the length of the circumference enclosing the detached region, and this length continuously increases as the peeling advances.

3.1 Double Peeling of a Tape

For the tape case, Fig. 3 shows the dimensionless load \hat{P} as a function of the detached length \hat{a}_{eq} at equilibrium, for different values of the work of adhesion $\Delta\hat{\gamma}$. The figure shows that the force constantly increases as the crack propagates. However, the trend shows an asymptotic behavior toward a limiting value \hat{P}_{lim} , which only depends on $\Delta\hat{\gamma}$. This is more clear in Fig. 4, where the load \hat{P} is

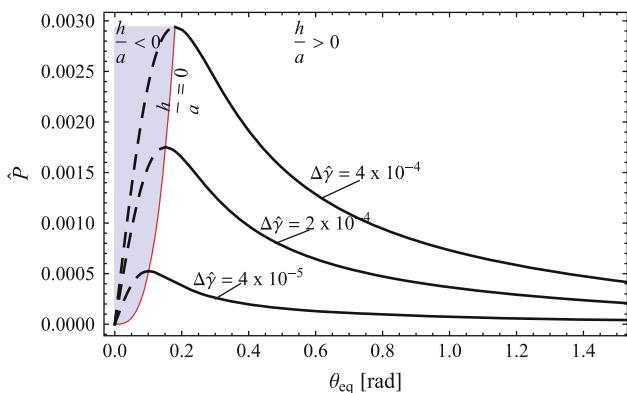


Fig. 4 The dimensionless peeling force \hat{P} as a function of the peeling angle θ_{eq} for an adhesive tape. Plots are given for different values of the dimensionless work of adhesion $\Delta\hat{\gamma}$

shown as a function of the peeling angle θ_{eq} at equilibrium. We note that the trend of the curves is in perfect agreement with the theoretical prediction presented in Ref. [37]. Interestingly, increasing the pull-off force determines, as expected, a decrease in the peeling angle. However, a lower bound θ_{lim} of the peeling angle exists at which the pull-off force takes its maximum value. Below this threshold value (see the gray area in Fig. 4), the condition 10 is violated and, therefore, the solution obtained for $\theta_{eq} < \theta_{lim}$ is physically meaningless, i.e., it is not admissible.

Figure 5 shows the quantity $\hat{\delta} = \delta/h$ at equilibrium as a function of θ_{eq} . Notice $\hat{\delta}$ diverges as θ_{eq} approaches to its lower bound $(\theta_{eq})_{lim}$. Hence, at the maximum pull-off force, the corresponding displacement is infinitely large: in the double peeling case, an endless tape can be detached by a finite force. The above arguments have implicitly assumed that $h > 0$. So one may wonder what happens when h is infinitely small, i.e., when $h \rightarrow 0$. This implies that also a is infinitely small because, for $\hat{P} < \hat{P}_{lim}$, the quantity $\hat{a}_{eq} = a_{eq}/h$ must be finite (see Fig. 3). As the applied load increases, the peeling angle constantly decreases. When $\theta_{eq} = \theta_{lim}$, the load no longer increases, i.e., the status of the system is uniquely identified by the conditions $\hat{P} = \hat{P}_{lim}$ and $\theta_{eq} = \theta_{lim}$. When this happens $\hat{a}_{eq} = a_{eq}/h$ diverges (see Fig. 3), therefore, being $h = 0$, the dimensional detached length a_{eq} takes a finite value, i.e., the tape starts to detach. Under this conditions, the equilibrium is “neutral,” and an infinitesimally small increment of \hat{P} above \hat{P}_{lim} causes the detached length a_{eq} to increase constantly until the tape completely detaches from the substrate. Notice that during this process, the displacement δ remains proportional to a through the relation $\delta = a_{eq} \tan \theta_{lim}$.

Figure 6, where the ratio $(\hat{\delta}/\hat{a})_{eq} = (\delta/a)_{eq}$ at equilibrium as a function of θ_{eq} is shown, clarifies this last point. As expected, at $\theta_{eq} = \theta_{lim}$, $(\delta/a)_{eq}$ reaches the limiting value $\tan \theta_{lim}$.

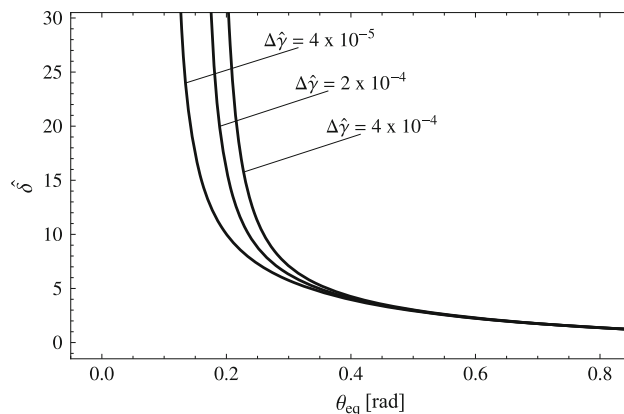


Fig. 5 The dimensionless displacement $\hat{\delta}$ as a function of the peeling angle θ_{eq} for an adhesive tape. Plots are given for different values of the dimensionless work of adhesion $\Delta\hat{\gamma}$

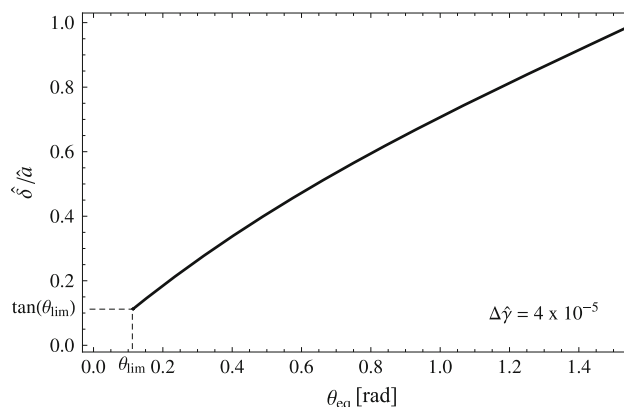


Fig. 6 The ratio $\hat{\delta}/\hat{a} = \delta/a$ as a function of the peeling angle θ_{eq} for an adhesive tape. Plot is given for $\Delta\hat{\gamma} = 4 \times 10^{-5}$. Observe that when $\theta_{eq} = \theta_{lim}$, $\delta/a = \tan \theta_{lim}$

The theoretical predictions presented so far agree very well with experiments carried on a standard adhesive tape adhered to a smooth flat Poly(methyl methacrylate) (PMMA) surface (see Ref. [67] for a detailed description of the setup and experimental procedure). The used tape was a Narpaint (NAR S.p.A. Reg. Imprese Padova C.F.) with a mean thickness of $125 \pm 12.5 \mu\text{m}$ and a width of 15 mm. Tensile tests of the tape were performed on 20 specimens of adhesive tape, using a testing machine (Insight 1 kN, MTS, Minnesota, USA), equipped with a 10 N cell load with pneumatic clamps in order to estimate the Young’s modulus of the tape itself. The computer program TestWorks 4 (MTS, Minnesota, USA) has been employed to acquire the experimental data of the tensile force applied and, then, the stress–strain curves were computed using the estimation of the real width and thickness at the cross-section of each specimen. Tests were recorded by a DCR SR55E SONY digital video camera, which allowed us to measure, with the aid of an ad hoc developed Matlab, ©

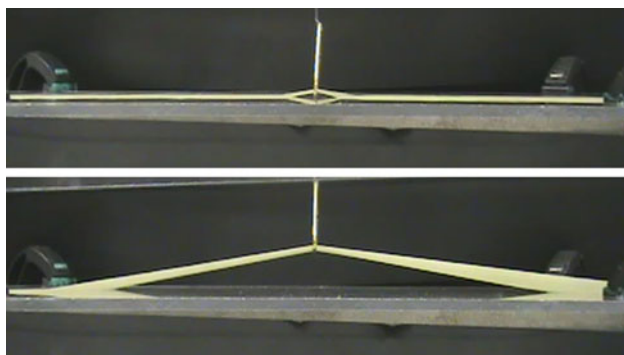


Fig. 7 Two frames recorded from experiments. The *upper picture* was taken at the beginning of the traction, and the *second* after few minutes

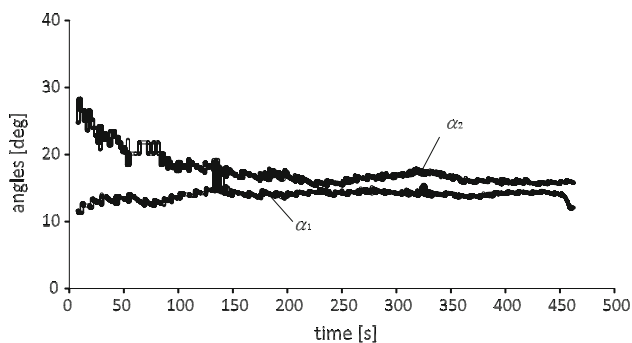


Fig. 8 The measured evolution of the left α_1 and right α_2 peeling angles during double peeling advance. Observe that the peeling angles rapidly stabilize on a almost constant limiting value θ_{lim} as indeed predicted by the theory

1994–2012 The MathWorks, Inc. code, the two peeling angles, respectively, at the left α_1 and right α_2 sides of the screen, see Fig. 7. Tests were performed starting with the adhesive tape which, at the beginning, was apparently fully adherent to the PMMA base. Figure 8 show how the measured peeling angles evolves as the double peeling advance. Observe that the two values of the peeling angles rapidly stabilize on a almost constant value θ_{lim} as indeed predicted by the theory. Noteworthy, the measured limiting angle θ_{lim} depends only $\Delta\hat{\gamma}$, and therefore, it can be used to indirectly measure the adhesion energy $\Delta\gamma$, given the geometric and elastic properties of the tape.

3.2 Axisymmetric Peeling of a Membrane

Now let us study the axisymmetric peeling of a initially flat infinitely large membrane. Figs. 9 and 10 show, at equilibrium, the dimensionless pull-off force \hat{P} and applied displacement $\hat{\delta}$ as a function of the dimensionless radius \hat{a}_{eq} of the detached area, for different values of the work of adhesion. Both the peeling force and displacement increase almost

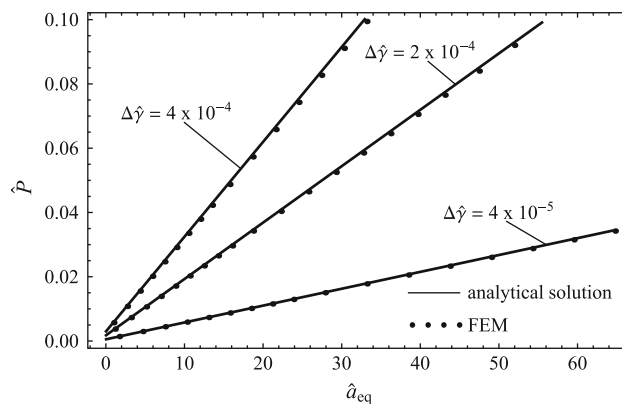


Fig. 9 The dimensionless peeling force \hat{P} as a function of the dimensionless detached length \hat{a}_{eq} for an adhesive membrane. Plots are given for different values of the dimensionless work of adhesion $\Delta\hat{\gamma}$. A comparison of the solution (*solid lines*) with FEM results (*dots*) is also shown

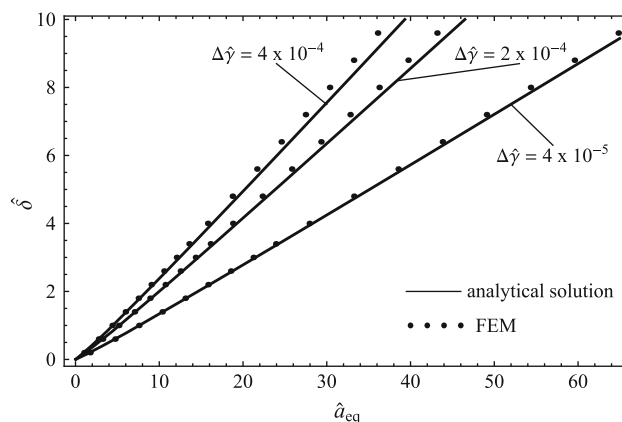


Fig. 10 The dimensionless applied vertical displacement $\hat{\delta}$ as a function of the dimensionless detached length \hat{a}_{eq} for an adhesive membrane. Plots are given for different values of the dimensionless work of adhesion $\Delta\hat{\gamma}$. A comparison of the solution (*solid lines*) with FEM results (*dots*) is also shown

linearly with the detached radius \hat{a}_{eq} . This simply leads to the conclusion that, as expected, the supported load is proportional to the length of the peeling line $l = 2\pi a_{eq}$ which, this time, increases linearly with the radius a_{eq} . Moreover, from Fig. 10, one also draws the conclusion that the peeling angle is, in this case, almost independent of the applied load. It only depends on the work of adhesion $\Delta\gamma$. The above arguments lead to the conclusion that a stable equilibrium condition is always found for any given applied load.

Results are also compared with those obtained with a finite element (FE) analysis carried out with the aid of the commercial software ANSYS [68]. In particular, axisymmetric shell elements have been adopted. Such elements are defined by two nodes and three degrees of freedom at each node: translations in the x , and y directions, and rotation about the z -axis corresponding to the

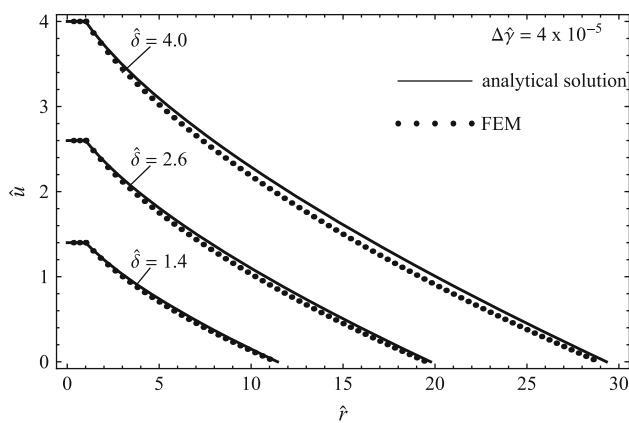


Fig. 11 The dimensionless deformed membrane profile $\hat{u}(\hat{r})$ for different values of the dimensionless applied displacement $\hat{\delta}$. Results are given for $\Delta\hat{\gamma} = 4 \times 10^{-5}$. A comparison with FEM results (dots) is also shown

circumferential direction. The membrane option has been employed, so the element uses one integration point through-the-thickness and accounts for only membrane stiffness (i.e., bending and transverse shear stiffness are ignored, and the rotational degree of freedom is excluded). The contact zone between the adhesive membrane and the flat rigid substrate is considered in sticking friction. This condition is taken into account by constraining the nodes on the adhering zone. Finite strain effects are taken into account by performing a large deflection analysis. To calculate, at prescribed displacement δ , the energy release rate, which occurs during the crack propagation, the following steps have been performed: (1) the detached radius a_i is fixed by constraining all nodes with radial coordinate larger than a_i , (2) the vertical displacement δ is applied to the nodes lying on the inner radius r_0 of the membrane, (3) the corresponding reaction force P and the elastic energy U_{el} stored in the system are calculated, then (4) the procedure is repeated for a new value of the detached radius $a_{i+1} = a_i + \Delta a$, given the same displacement δ . The energy release rate G for each a_i is hence calculated as:

$$G_i = -\frac{\Delta U_{el}}{\Delta S} = -\frac{1}{\pi} \frac{U_{el,i+1} - U_{el,i}}{a_{i+1}^2 - a_i^2} \quad (25)$$

Finally, the detached radius at the equilibrium is evaluated by enforcing the Griffith equation (1).

Notwithstanding the assumptions employed to formulate the problem, the agreement between our analytical solution and the fully numerical one is very good. In particular, in terms of pull-off force, analytical results are only a few percentage points different from the FEM ones.

Figure 11 shows the dimensionless deformed profile of the membrane for different values of the dimensionless

applied displacement $\hat{\delta}$ and a work of adhesion $\Delta\hat{\gamma} = 4 \times 10^{-5}$. FEM results are also plotted for comparison. The membrane profile predicted by (18) slightly deviates from the numerical results, leading to a slight overestimation of the profile height distribution. Interestingly, this small mismatch very negligibly affects the prediction of the pull-off force (see Fig. 9).

We observe that a discontinuity in the peeling line caused by the presence of a defect under the contact zone would determine a decrease in the supporting load capacity of the membrane in the zone perturbed by the defect. However, in the unperturbed regions, the peeling line would not be interrupted by defects, and the loading capacity of the system would remain necessarily unchanged.

4 Conclusions

The mechanism of detachment of thin films adhering to a rigid substrate has been investigated. We have proposed a comparison between the double peeling of an elastic endless tape and the axisymmetric peeling of an elastic membrane. In particular, for the membrane case, a simplified approach, based on the assumption of negligible radial displacements and small deformations, has been developed leading to a very good agreement with results obtained by large deformation numerical calculations.

In the case of tape case, a lower bound θ_{lim} of the peeling angle exists at which the pull-off force P takes its maximum value P_{lim} , i.e., a further increase in P above P_{lim} causes the detachment of the entire tape. These results agree with the theory of multiple peeling and clarify some aspect of this theory. Moreover, the theoretical predictions have been confirmed by experiments.

The mechanism of detachment of a thin membrane is substantially different, since, in this case, the peeling line increases linearly with the radius of the detached area, leading to an almost proportional increase in the supported load. We, indeed, find that, in the case of membrane peeling, the mechanism of detachment is always stable, i.e., the membrane can sustain, in principle, any applied load, the limit being only represented by the strength of the material. Moreover, the theoretical predictions have been confirmed by FEM simulations.

Acknowledgments The authors acknowledge Regione Apulia and the Italian Ministry of Education, University and Research for having supported the research activity within the project TRASFORMA Laboratory Network cod. 28, and projects PON01_02238 and PON02_00576_3333604. This work is also supported by the ERC

Ideas Starting Grant No. 279985 ‘BIHSNAM—Bio-Inspired Hierarchical Super Nanomaterials’ and by the ERC Proof of Concept REPLICA (both PI Nicola Pugno).

References

- Steinberg, M.S.: On the mechanism of tissue reconstruction by dissociated cells: I. Population kinetics, differential adhesiveness, and the absence of directed migration. *Proc. Natl. Acad. Sci. U. S. A.* **48**, 1577–1582 (1962)
- Steinberg, M.S.: Mechanism of tissue reconstruction by dissociated cells: II. Time course of events. *Science* **137**, 762–763 (1962)
- Steinberg, M.S.: On the mechanism of tissue reconstruction by dissociated cells: III. Free energy relations and the reorganization of fused, heteronomic tissue fragments. *Proc. Natl. Acad. Sci. U. S. A.* **48**, 1769–1776 (1962)
- Lackie, J.M.: *The Dictionary of Cell & Molecular Biology*. Academic Press, (2013)
- Geim, A.K., Dubonos, S.V., Grigorieva, I.V., Novoselov, K.S., Zhukov, A.A., Shapova, S.Y.: Microfabricated adhesive mimicking gecko foot-hair. *Nat Mater* **2**, 461–463 (2003)
- Pugno, N.M.: Towards a Spiderman suit: large invisible cables and self-cleaning releasable super-adhesive materials. *J Phys Cond Mat* **19**, 395001 (2007)
- Pugno, N.M.: Spiderman gloves. *Nano Today* **3**, 35–41 (2008)
- Autumn, K., Sitt, M., Liang, Y.A., Peattie, A.M., Hansen, W.R., Sponberg, S., Kenny, T.W., Fearing, R., Israelachvili, J.N., Full, R.J.: Evidence for van der Waals adhesion in gecko setae. *Proc Natl Acad Sci USA* **99**, 12252–12256 (2002)
- Kendall, K.: Thin-film peeling—the elastic term. *J.Phys. D: Appl Phys* **8**, 1449–1452 (1975)
- Varenberg, M., Pugno, N., Gorb, S.: Spatulate structures in biological fibrillar adhesion. *Soft Matter* **6**, 3269–3272 (2010)
- Scherge, M., Gorb, S.N.: *Biological micro- and nanotribology*. Springer, (2001)
- Glassmaker, N.J., Jagota, A., Hui, C.-Y., Noderer, W.L., Chaudhury, M.K.: Biologically inspired crack trapping for enhanced adhesion. *Proc. Natl. Acad. Sci. USA* **104**, 10786–10791 (2007)
- Carbone, G., Mangialardi, L., Persson, B.N.J.: Adhesion between a thin elastic plate, and a hard randomly rough substrate. *Physical Review B* **70**(12), 125407 (2004)
- Ding, J., Meng, Y., Wen, S.: Mechanical Stability and Sticking in a Model Microelectromechanical systems (MEMS) under Casimir Forces—Part II: The Role of the Casimir Effect. *International Journal of Nonlinear Sciences and Numerical Simulation* **1**, 379–384 (2000)
- Ding, J., Wen, S., Meng, Y.: Theoretical study of the sticking of a membrane strip in MEMs under the Casimir effect. *J Micromech Microeng* **11**, 202–208 (2001)
- Linder, C., Rooji, N.F.D.: Investigating on free-standing polysilicon beams in view of their applications as transducers. *Sensors and Actuators A (Physical)* **21**(23), 1053–1059 (1990)
- Israelachvili, J.N., Tabor, D.: The measurement of van der Waals dispersion forces in the range 1.5 to 130 nm. *Proc. R. Soc. A* **331**, 19–38 (1972)
- Tas, N., Sonnenberg, T., Jansen, H., Legtenberg, R., Elwenspoek, M.: Sticking in surface micromachining. *J Micromech Microeng* **6**, 385–397 (1996)
- Shanahan, M.E.R.: A variant of JKR test- a slightly inflated balloon. *CR. Acad. Sci. Ser. II-B* **321**, 259–264 (1995)
- Shanahan, M.E.R.: A novel test for the appraisal of solid/solid interfacial interactions. *J Adhesion* **63**, 15–29 (1997)
- Shanahan, M.E.R.: Adhesion of a punch to a thin membrane. *CR Acad Sci Ser IV* **1**, 517–522 (2000)
- Wan, K.T.: Adherence of an axisymmetric flat punch on a flexible membrane. *J Adhesion* **75**, 369–380 (2001)
- Wan, K.T.: Adherence of an axisymmetric flat punch onto a clamped circular plate: transition from a rigid plate to a flexible membrane. *J Appl Mech* **69**, 104–109 (2002)
- Wan, K.T., Dillard, D.A.: Adhesion of a flat punch adhered to a thin pre-stressed membrane. *J Adhesion* **79**, 123–140 (2003)
- Plaut, R.H., White, S.A., Dillard, D.A.: Effect of work of adhesion on contact of a pressurized blister with a flat surface. *Int J Adhesion* **23**, 207–214 (2003)
- Jin, C.: Theoretical study of mechanical behavior of thin circular film adhered to a flat punch. *Int J Mech Sci* **51**, 301–313 (2009)
- Plaut, R.H.: Linearly elastic annular and circular membranes under radial, transverse, and torsional loading. Part: I large unwrinkled axisymmetric deformations. *Acta MEch* **202**, 79–99 (2009)
- Nadler, B., Tang, T.: Decohesion of a rigid punch from non-linear membrane undergoing finite axisymmetric deformation. *Int J Non-Linear Mech* **43**, 716–721 (2008)
- LongR. Hui, C-Y.: Axisymmetric membrane in adhesive contact with rigid substrates: Analytical solutions under large deformation. *Int J Sol Struct* **49**, 672–683 (2012)
- Foster, O.H.: Very large deformations of axially symmetrical membranes made of neo-Hookean materials. *Int J Eng Sci* **5**, 95–117 (1967)
- Autumn, K., Peattie, A.M.: Mechanisms of Adhesion in Geckos. *Int Comp Biol* **42**, 1081–1090 (2002)
- Autumn, K., Dittmore, A., Santos, D., Spenko, M., Cutkosky, M.: Frictional adhesion: a new angle on gecko attachment. *J Exp Biol* **209**, 3569–3579 (2006)
- Autumn, K., Hsieh, S.T., Dudek, D.M., Chen, J., Chitaphan, C., Full, R.J.: Dynamics of geckos running vertically. *J Exp Biol* **209**, 260–272 (2006)
- Gravish, N., Wilkinson, M., Autumn, K.: Frictional and elastic energy in gecko adhesive detachment. *J R Soc Interface* **6**, 339–348 (2008)
- Tian, Y., Pesika, N., Zeng, H., Rosenberg, K., Zhao, B., McGuiggan, P., Autumn, K., Israelachvili, J.N.: Adhesion and friction in gecko toe attachment and detachment. *Proc Natl Acad Sci USA* **103**, 19320–19325 (2006)
- Pesika, N.S., Tian, Y., Zhao, B., Rosenberg, K., Zeng, H., McGuiggan, P., Autumn, K., Israelachvili, J.N.: Peel-Zone Model of Tape Peeling Based on the Gecko Adhesive System. *J Adhesion* **83**(4), 383–401 (2007)
- Pugno, N.M.: The theory of multiple peeling. *Int J Fract* **171**, 185–193 (2011)
- Spolenak, R., Gorb, S., Gao, H.J., Arzt, E.: Effects of contact shape on the scaling of biological attachments. *Proc R Soc London Ser A* **461**, 305–319 (2005)
- del Campo, A., Greiner, C., Artz, E.: Adhesion of bioinspired micropatterned surfaces: Effects of pillar radius, aspect ratio, and preload. *Langmuir* **23**, 10235–10243 (2007)
- Chung, J.Y., Chaudhury, M.K.: Roles of discontinuities in bioinspired adhesive pads. *J R Soc Interface* **2**, 55–61 (2005)
- Barthlott, W., Neinhuis, C.: Purity of the sacred lotus or escape from contamination in biological surfaces. *Planta* **202**, 1–8 (1997)
- Martines, E., Seunarine, K., Morgan, H., Gadegaard, N., Wilkinson, C.D.W., Riehle, M.O.: Superhydrophobicity and Superhydrophilicity of Regular Nanopatterns. *Nano Lett* **5**, 2097–2103 (2005)
- Callies, M., Chen, Y., Marty, F., Pepin, A., Quere, D.: Microfabricated textured surfaces for super-hydrophobicity investigations. *Microelectron Eng* **78/79**, 100–105 (2005)

44. Afferrante, L., Carbone, G.: Microstructured superhydrorepellent surfaces: effect of drop pressure on fakir-state stability and apparent contact angles. *J. Phys. Condens. Matter* **22**, 325107 (2010)
45. Fearing, J.N.: Gecko adhesion bibliography. Department of EECS, University of California, Berkeley (2008). See <http://robotics.eecs.berkeley.edu>.
46. Autumn, K., Liang, Y.A., Hsieh, S.T., Zesch, W., Chan, W.-P., Kenny, W.T., Fearing, R., Full, R.J.: Adhesive force of a single gecko foot-hair. *Nature* **405**, 681–685 (2000)
47. Lepore, E., Pugno, F., Pugno, N.M.: Optimal Angles for Maximal Adhesion in Living Tokay Geckos. *The J of Adh* **88**, 820–830 (2012)
48. K, C., Zheng, M., Zhou, G., Cui, W., Pugno, N., Miles, R.M.: Mechanical peeling of free-standing single-walled carbon-nanotube bundles. *Small* **6**(3), 438–445 (2010)
49. Gao, H.J., Wang, X., Yao, H.M., Gorb, S., Arzt, E.: Mechanics of hierarchical adhesion structures of geckos. *Mech Mater* **37**, 275–285 (2005)
50. Kim, T.W., Bhushan, B.: Effect of stiffness of multi-level hierarchical attachment system on adhesion enhancement. *Ultramicroscopy* **107**, 902–912 (2007)
51. Autumn, K., Majidi, C., Groff, R., Dittmore, A., Fearing, R.: Effective elastic modulus of isolated gecko setal arrays. *J Exp Biol* **209**, 3558–3568 (2006)
52. Pugno, N.M., Cranford, S.W., Buehler, M.J.: Synergetic Material and Structure Optimization Yields Robust Spider Web Anchorages. *SMALL* **9**(16), 2747–2756 (2013)
53. Carbone, G., Pierro, E., Gorb, N.: Origin of the superior adhesive performance of mushroom-shaped microstructured surfaces. *Soft Matter* **7**, 5545–5552 (2011)
54. Carbone, G., Pierro, E.: Sticky bio-inspired micropillars: Finding the best shape. *SMALL* **8**(9), 1449–1454 (2012)
55. Afferrante, L., Carbone, G.: Biomimetic surfaces with controlled direction-dependent adhesion. *J R Soc Interface* **9**, 3359–3365 (2012)
56. Carbone, G., Pierro, E.: Effect of interfacial air entrapment on the adhesion of bio-inspired mushroom-shaped micro-pillars. *Soft Matter* **8**, 7904–7908 (2012)
57. Carbone G., Pierro E.: A review of adhesion mechanisms of mushroom-shaped microstructured adhesives. *Meccanica* (2013). doi:10.1007/s11012-013-9724-9
58. Afferrante, L., Carbone, G.: The mechanisms of detachment of mushroom-shaped micro-pillars: from defect propagation to membrane peeling. *React Eng* (2013). doi:10.1002/mren.201300125
59. Fuller, K.N.G., Tabor, D.: The Effect of Surface Roughness on the Adhesion of Elastic Solids. *Proc. R. Soc. Lond. A* **345**(1642), 327–342 (1975)
60. Greenwood, J.A., Williamson, J.B.P.: Contact of nominally flat surfaces. *Proc R Soc Lond A* **295**, 300–319 (1966)
61. Carbone, G., Bottiglione, F.: Asperity contact theories: Do they predict linearity between contact area and load?. *Journal of the Mechanics and Physics of Solids* **56**, 2555–2572 (2008)
62. Putignano, C., Afferrante, L., Carbone, G., Demelio, G.: A new efficient numerical method for contact mechanics of rough surfaces. *International Journal of Solids and Structures* **9**(2), 338–343 (2012)
63. Putignano, C., Afferrante, L., Carbone, G., Demelio, G.: The influence of the statistical properties of self-affine surfaces in elastic contact: a numerical investigation. *Journal of the Mechanics and Physics of Solids* **60**, 973–982 (2012)
64. Putignano, C., Afferrante, L., Carbone, G., Demelio, G.: A multiscale analysis of elastic contacts and percolation threshold for numerically generated and real rough surfaces. *Tribology International* **64**, 148–154 (2013)
65. Afferrante, L., Carbone, G., Demelio, G.: Interacting and coalescing Hertzian asperities: a new multiasperity contact model. *Wear* **278**(–279), 28–33 (2012)
66. Maugis, D.: *Contact, Adhesion and Rupture of Elastic Solids*, Springer Series in Solid State Sciences. Springer-Verlag, Berlin, Heidelberg, New-York (1999)
67. Lepore, E., et al.: Experiments on multiple peeling. In preparation.
68. ANSYS, ANSYS User's Manual, Version 14.5